Modular chemical mechanism predicts spatiotemporal dynamics of initiation in the complex network of hemostasis

Christian J. Kastrup, Matthew K. Runyon, Feng Shen, and Rustem F. Ismagilov*

Department of Chemistry and Institute for Biophysical Dynamics, University of Chicago, 929 West 57th Street, Chicago, IL 60637

Edited by George M. Whitesides, Harvard University, Cambridge, MA, and approved August 30, 2006 (received for review July 3, 2006)

This article demonstrates that a simple chemical model system, built by using a modular approach, may be used to predict the spatiotemporal dynamics of initiation of blood clotting in the complex network of hemostasis. Microfluidics was used to create *in vitro* environments that expose both the complex network and the model system to surfaces patterned with patches presenting clotting stimuli. Both systems displayed a threshold response, with clotting initiating only on isolated patches larger than a threshold size. The magnitude of the threshold patch size for both systems was described by the Damköhler number, measuring competition of reaction and diffusion. Reaction produces activators at the patch, and diffusion removes activators from the patch. The chemical model made additional predictions that were validated experimentally with human blood plasma. These experiments show that blood can be exposed to significant amounts of clot-inducing stimuli, such as tissue factor, without initiating clotting. Overall, these results demonstrate that such chemical model systems, implemented with microfluidics, may be used to predict spatiotemporal dynamics of complex biochemical networks.

complexity | microfluidics | networks | tissue factor | nonlinear

Complex networks of interacting reactions are responsible for the function and self-regulation of biological systems and are the focus of a substantial research effort (1–8). The spatiotemporal dynamics of such networks (2, 4) is especially challenging and interesting to understand, and to reproduce in synthetic model systems (2, 3, 5, 9–11). Simplified physical or chemical model systems are attractive for understanding biological complexity because these models can be made simple to probe, analyze, and understand. These models, even if correct, may be met with skepticism that "there is no model simpler than life itself" (12), unless predictions can be made with the model system and can be tested and validated with the complex network. This testing is often difficult for experimental models of spatiotemporal dynamics because both the model system and the complex network must be perturbed and observed in space and time in a controlled fashion.

In this article, we use soft lithography and microfluidics (13) to control and compare the spatiotemporal dynamics of two networks: the complex network of hemostasis and a simple chemical model system that describes the network. Our main question is whether the qualitative dynamics of the complex network may be predicted by observing the dynamics of this "analogue" model system, and whether semiquantitative scaling predictions can be made to relate the dynamics of the two systems. To control clotting, the network of ≈80 reactions (14) of hemostasis must be robust: it must initiate blood clotting at a patch of substantial vascular injury but not at patches of smaller damage that are believed to be present throughout the vascular system (15, 16). Although most of the individual reactions in hemostasis have been characterized, its overall spatiotemporal dynamics remains less understood (17) because the system is complex. The function of hemostasis has been postulated to depend on the delicate balance of production, consumption, and transport—by diffusion or by convective flow—of clotting factors (14, 15, 17–19). Modeling all reactions together with transport phenomena is exceptionally challenging. As is typical for complex networks, many models are proposed to describe hemostasis but are not readily accepted (12). Even the most basic aspects of threshold dynamics of hemostasis remain under debate, such as whether blood can be exposed to clot-inducing stimuli, including tissue factor, without initiating clotting (20, 21, 46). In this article, we use microfluidics to expose the two networks to surfaces patterned with patches presenting clotting stimuli. We perform this comparison of the spatiotemporal dynamics of initiation in these two networks in the absence of convective transport (fluid flow) to make the analysis unambiguous and to avoid complicating effects such as eddies and turbulent flow present at high values of the Reynolds number (22).

To model the spatiotemporal dynamics of initiation, we simplified the complexity of the hemostasis network so both reactions and transport could be analyzed intuitively. We represented (18) ≈80 reactions of hemostasis as three interacting modules (5), with the overall kinetics corresponding to (*i*) higher-order autocatalytic production of activators, (*ii*) linear consumption of activators, and (*iii*) formation of the clot at high concentrations of activators. Concentration of activators, C, acted as a control parameter. Interactions among these modules lead to a threshold concentration, C_{thresh}, above (but not below) which clotting was initiated. In this representation, hemostasis is normally in the stable steady state at low C. Small increases of C preserve $C < C_{\text{thresh}}$, such perturbations decay, and the system returns to the stable steady state. Large perturbations increase the concentration above the unstable steady state ($C > C_{\text{thresh}}$), resulting in amplification of activators and initiation of clotting. This representation does not require knowledge of all of the reactions of clotting, but it is consistent with the known kinetics of hemostasis (e.g., autocatalytic loops are involved in activation of clotting). Here, we did not attempt to map all reactions of hemostasis onto modules. We hypothesized that a functional, but drastically simplified, chemical model of hemostasis may be created by replacing each module with at least one chemical reaction with kinetics matching that of the module. We previously used organic and inorganic reactions (23) to create such a system and to model spreading of clotting through junctions of vessels (18). This system used acid (the hydronium ion H_3O^+) as the activator of gelling, or "clotting." The clotting reaction was monitored by observing the transition of the reaction mixture from basic to acidic, which caused gelling of alginic acid and changed the color

Author contributions: C.J.K., M.K.R., and R.F.I. designed research; C.J.K., M.K.R., and F.S. performed research; C.J.K. and M.K.R. contributed new reagents/analytic tools; C.J.K., M.K.R., F.S., and R.F.I. analyzed data; and C.J.K., M.K.R., and R.F.I. wrote the paper.

The authors declare no conflict of interest.

This article is a PNAS direct submission.

Abbreviation: TF, tissue factor.

See Commentary on page 15727.

*To whom correspondence should be addressed. E-mail: r-ismagilov@uchicago.edu.

© 2006 by The National Academy of Sciences of the USA

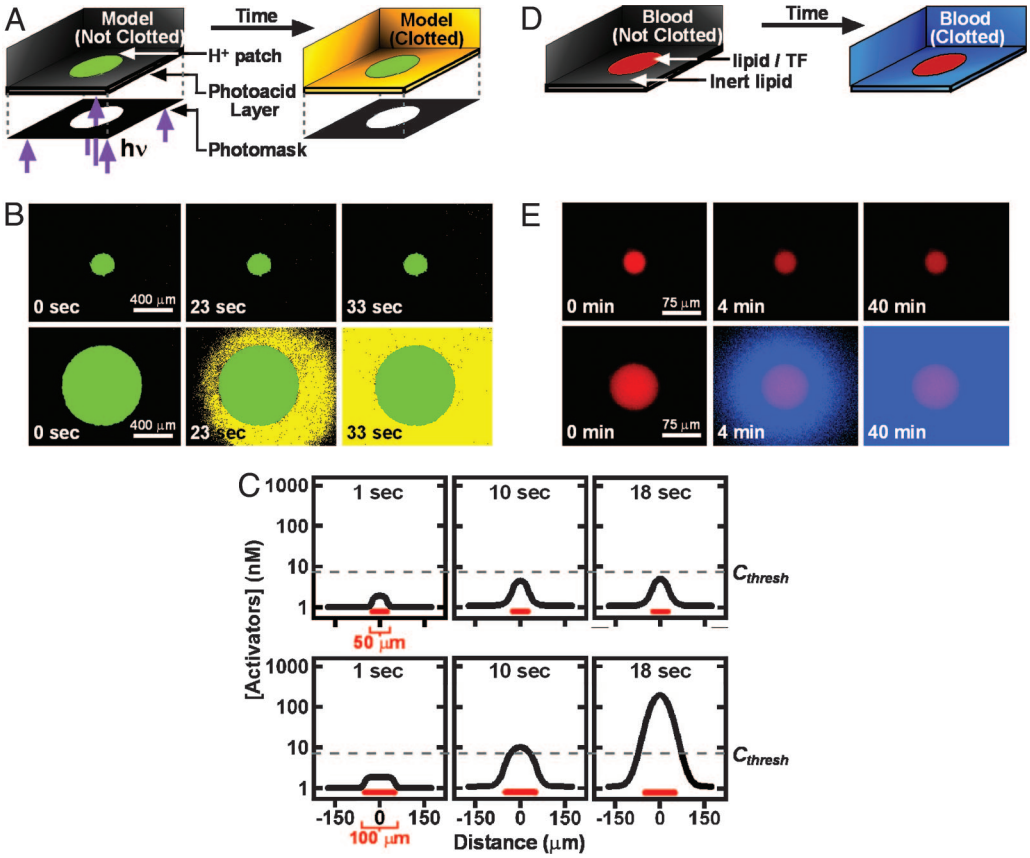

Fig. 1. Human blood plasma and the simple chemical model both initiate clotting with a threshold response to the size of patches presenting clotting stimuli. (*A*) Simplified schematic of a microfluidic device used to test threshold response in initiation of clotting in the chemical model. The reaction mixture was kept over a photoacid surface containing 2-nitrobenzaldehyde. UV irradiation through a photomask photoisomerized 2-nitrobenzaldehyde (not acidic) to 2-nitrosobenzoic acid (acidic, $pK_a < 4$), creating acidic patches of clotting stimuli (green). When clotting was initiated, the basic reaction mixture became acidic and turned yellow (see the supporting information). (*B*) Time-lapse fluorescent micrographs of initiation of clotting (false-colored yellow) in the chemical model on patches $p = 200$ μm (*Upper*, no initiation) and $p = 800$ μm (*Lower*, rapid initiation). (*C*) Numerical simulations qualitatively describing the competition between production of clotting activators at the patch (red) and diffusion of activators away from the patch in regulating initiation of clotting (see the supporting information). For subthreshold patches (*Upper*, 50 μm) diffusion dominates and the concentration of activators never reaches the threshold concentration C_{thresh} (dashed line) necessary to initiate clotting. For above-threshold patches (*Lower*, 100 μm), the production of activators dominates, exceeding C_{thresh}, leading to rapid amplification of activators and initiation of clotting. (*D*) Schematic of an *in vitro* microfluidic system used to contain blood plasma and to expose it to patches presenting clotting stimuli. Patches of negatively charged phospholipid bilayers with reconstituted tissue factor (lipid/TF; red fluorescence) were patterned in a background of inert lipids. Blue represents clotting. (*E*) Time-lapse fluorescent micrographs of initiation of clotting (blue fluorescence) of blood plasma on red patches $p = 50$ μm (*Upper*, no initiation) and $p = 100$ μm (*Lower*, rapid initiation), where p [m] is the diameter of the patch.

of a pH indicator. Here, we directly compare the spatiotemporal dynamics of the model system and the complex network, testing whether the chemical model can successfully reproduce and predict the dynamics of initiation of clotting.

Results

Initiation of Clotting in the Chemical Model Showed a Threshold Response to Patch Size. To observe the qualitative dynamics of this chemical model system, we tested whether initiation of clotting on acidic patches was robust (initiating on large but not small patches) (Fig. 1*A*). UV light was used as a stimulus for initiating clotting. Photochemical production of acid (24) was spatially confined to patches by using a photomask and acid diffused from the surface patch into the solution. The clotting reaction was initiated only if the local concentration of acid exceeded the threshold value C_{thresh}. Initiation of clotting in the chemical model showed a threshold response to patch size, p [m], the diameter of a circular patch (Fig. 1*B*, 17 experiments). Single patches $p \geq 400 \geq p_{tr}$ μm reliably initiated clotting in ≈22 s, whereas single patches $p \leq 200 < p_{tr}$ μm did not cause initiation within 500 s. Control experiments (see the supporting information, which is published on the PNAS web site) verified that initiation was due to the production of acid at the surface and not due to heating of the sample or photochemistry of the solution.

Initiation of Clotting in the Chemical Model May Be Described by the Damköhler Number. To obtain a semiquantitative description of the dynamics in this system, we estimated the threshold patch size, p_{tr} [m] (size p of the smallest patch that initiates clotting), by considering the competition of reaction and diffusion. Reaction produces an activator at the patch on the time scale t_R [s], and diffusive transport removes the activator from the patch on the time scale t_D [s]. For patches $p < p_{tr}$ diffusion dominates ($t_D < t_R$), and the concentration of activator never reaches the threshold C_{thresh}. For patches $p > p_{tr}$, reaction dominates ($t_D > t_R$), local concentration of activator exceeds the threshold C_{thresh}, and clotting is initiated. This competition is described by the Damköhler number (22), where p_{tr} corresponds to p at which $t_R \approx t_D$ (Fig. 1*C*). Since $t_D \approx p^2/D$, p_{tr} should scale as $p_{tr} \approx (D \times t_R)^{1/2}$, where D [$m^2 \cdot s^{-1}$] is the diffusion coefficient of the activator. This scaling prediction is reasonable and is consistent with the one originally proposed for membrane patch size

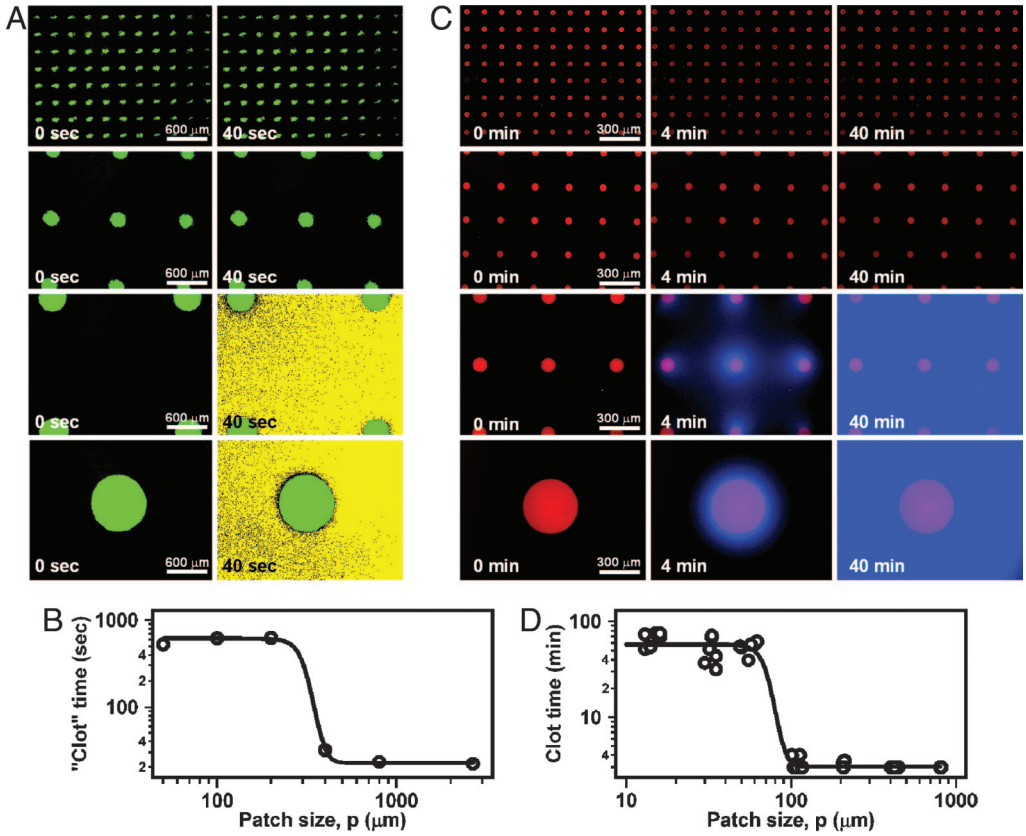

Fig. 2. Chemical model correctly predicts that *in vitro* initiation of clotting in human blood plasma depends on the spatial distribution, rather than the total surface area of a lipid surface presenting TF, a clotting stimulus. (*A*) Time-lapse fluorescent micrographs of initiation of clotting (yellow) in the chemical model on arrays of patches, $p = 50$, 200, 400, and 800 μm (top to bottom, green). All arrays had the same total surface area of patches (5×10^5 μm^2). Clotting did not initiate on arrays of patches $p = 50$–200 μm but rapidly initiated on patches $p = 400$–800 μm. (*B*) Graph quantifying the threshold response for initiation of clotting in the chemical model, using data as shown in *A*. (*C*) Time-lapse fluorescent micrographs showing initiation of clotting (blue) of blood plasma on arrays $p = 100$ μm and $p = 400$ μm patches (red), but no initiation on arrays of $p = 25$ μm and $p = 50$ μm patches (red). The total surface area of patches in all arrays was the same (3.5×10^6 μm^2). (*D*) Graph quantifying the threshold response for initiation of clotting of blood plasma using data as shown in *C*. Clot times were determined by monitoring the appearance of fibrin.

regulating a proteolytic feedback loop on a membrane during clotting (15). For the chemical model system, experimental value $200 < p_{tr} < 400$ μm agreed with predicted $p_{tr} \sim 470$ μm, calculated by using $D(H^+) \sim 10^{-8}$ m^2·s^{-1} and $t_R \sim 22$ s.

The Chemical Model Correctly Predicts the Spatiotemporal Dynamics for *in Vitro* Initiation of Clotting. This chemical model makes four predictions for initiation of blood clotting. First, it predicts the existence and the value of the threshold patch size, p_{tr}. To test this prediction and to probe the dynamics of initiation of the hemostasis network, we developed an *in vitro* microfluidic system to control initiation of clotting in space and time (Fig. 1*D*). We used patterned supported phospholipid bilayers (25, 26) to present patches of the clotting stimulus, a lipid surface containing phosphatidylserine with reconstituted human tissue factor (TF) (27, 28). TF was incorporated into bilayers as previously described (27, 28). TF is an integral membrane protein that is exposed at sites of vascular damage and atherosclerotic plaque rupture (15, 16). These clot-inducing patches were surrounded by background areas of inert lipid bilayers (phosphatidylcholine). We used a microfluidic chamber to contain freshly recalcified plasma over the patterned lipid surface and to eliminate convection. Initiation in the hemostasis network may occur through two pathways: the TF pathway and the factor XII pathway. Corn trypsin inhibitor was used to inhibit the factor XII pathway (29) in experiments testing initiation by TF. We and others (27) refer to "initiation" in this network as the clotting process that culminates in a spike of thrombin and the onset of fibrin formation. We used bright-field microscopy to detect formation of fibrin and fluorescence microscopy to detect thrombin-induced cleavage of a peptide-modified coumarin dye (29).

Initiation of clotting of blood plasma in this microfluidic system displayed a threshold response to patch size. Patches $p \geq 100$ μm initiated clotting in <3 min (40 of 44 experiments), whereas patches $p \leq 50$ μm did not initiate clotting (28 of 28 experiments; at least 30 patches per experiment) (Fig. 1*E*). Background clotting was observed in 32–75 min in experiments with patches $p \leq 50$ (generally initiating not on the patches), consistent with the 45–70 min range for initiation on surfaces that had no patches at all and with the background clotting times reported by others (29). Initiated clotting spread as a reactive front at 25–35 μm/min. To predict the value of p_{tr}, we used $D \sim 5 \times 10^{-11}$ m^2·s^{-1} [approximate value for thrombin (30) as a representative activating protein involved in the amplification of the clotting cascade] and $t_R \sim 30 \pm 5$ s (obtained by measuring the initiation time of clotting on a nonpatterned clot-inducing bilayer). Predicted $p_{tr} \sim 40$ μm agreed with the measurement $50 < p_{tr} < 100$ μm. A considerably smaller threshold patch size (few micrometers) was previously proposed by considering diffusion of an activator in a membrane (15). Our results indicate that p_{tr} is determined by diffusion of a protein in solution.

Second, the model predicts that the size of individual patches (isolated, noninteracting), rather than their total surface area,

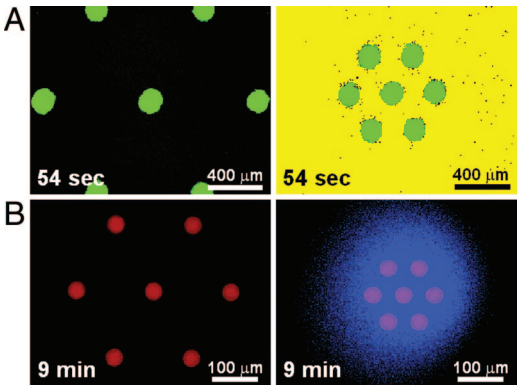

Fig. 3. Chemical model correctly predicts that initiation of clotting of human blood plasma can occur on tight clusters of subthreshold patches that communicate by diffusion. (*A*) Fixed-time (54 s) fluorescent micrographs of clusters of subthreshold patches $p = 200$ μm (green) in the chemical model system. These patches initiated clotting (yellow) when separated by 200 μm (*Right*) but not 800 μm (*Left*). (*B*) Fixed-time (9 min) fluorescent micrographs of clusters of subthreshold patches $p = 50$ μm (red) exposed to blood plasma. In agreement with the prediction (see text for details), these patches initiated clotting (blue) when separated by 50 μm (*Right*) but not 200 μm (*Left*).

determines initiation of clotting. To demonstrate this effect, we exposed the chemical model to arrays of patches (Fig. 2 *A* and *B*). Each array had the same total surface area of patches (5×10^5 μm^2) and produced the same amount of acid, but only arrays with individual patches $p \geq 400$ μm initiated clotting. Total area was irrelevant: a single patch above the threshold size quickly initiated clotting, whereas an array of subthreshold patches with a total surface area four times larger and producing approximately four times more acid did not (see the supporting information). Clotting of blood plasma (Fig. 2 *C* and *D*) also displayed this dynamics: among arrays of patches of the same total surface area, only arrays with patches $p \geq 100$ μm initiated clotting (six measurements per patch size). Initiation of clotting was exquisitely sensitive to the spatial distribution of TF in the sample. Knowing the amount of TF in the sample was not sufficient to predict whether initiation would occur; in our experiments with constant volumes of blood plasma, above-threshold patches induced clotting, whereas an array of subthreshold patches with a total surface area 20 times larger, bearing 20 times more TF, did not.

Third, the model predicts that a sufficiently tight cluster of subthreshold patches should initiate clotting (Fig. 3). Production of the activator on patches at the perimeter of the cluster reduces the diffusive flux of the activators away from the central patch. For a given t_R, initiation of clotting should occur for subthreshold patches spaced closer than the diffusion length scale, equal to p_{tr}. To demonstrate this effect, we exposed the chemical model ($200 < p_{tr} < 400$) to two clusters of subthreshold patches (Fig. 3*A*). Clusters of 200-μm patches separated by 200 μm rapidly initiated clotting, whereas clusters separated by 800 μm did not. Numerical simulations agreed with these experiments (see the supporting information). We verified these predictions with blood plasma ($50 < p_{tr} < 100$), where clusters of 50-μm patches separated by 50 μm rapidly initiated clotting and clusters of 50 μm patches separated by 200 μm did not (nine experiments) (Fig. 3*B*). It is known that amplification of activators could happen much more rapidly on the surfaces of membranes, especially of platelets (31), and these results further confirm the importance of transport in solution in setting p_{tr}.

Fourth, if this chemical model represents the overall dynamics of initiation in the network, rather than a subset of reactions in the TF pathway, it suggests that initiation of blood clotting via the factor XII pathway would also show a threshold response. To initiate this pathway, we exposed blood plasma to negatively charged glass, and initiation occurred in $t_R \sim 9$ min. We used the diffusion coefficient for thrombin to predict the threshold patch size $p_{tr} \sim (D \times t_R)^{1/2} \sim 160$ μm. To test this prediction, we created patches of hydrophilic glass in a background of inert, hydrophobic silanized glass (32). We rapidly determined $p_{tr} \sim 100$ μm by placing blood plasma on a single array of patches of different sizes (Fig. 4). In all 14 experiments, patches $p \geq 200$ μm induced clotting, but patches $p \leq 50$ μm did not. Patches $p = 100$ μm were close to threshold size, initiating clotting (12–19 min) in only 4 of 14 experiments, consistent with either slight variations of the surface chemistry from patch to patch or the stochastic nature (29) of the initiation of clotting via the factor XII pathway. These experiments indicate that the ability of a patient's blood to initiate clotting by either the TF or factor XII pathways can be rapidly evaluated by measuring the threshold response on a single slide with an array of patches of different sizes (e.g., Fig. 4).

Discussion

We focused on comparing the dynamics of initiation of clotting in a chemical model system and the complex biochemical network under *in vitro* conditions carefully controlled with microfluidics. We described experiments performed on flat surfaces in the absence of fluid flow. The effect of curvature of the surfaces should be important for patches in small capillaries, and further experiments and 3D simulations are needed to understand this effect. Nevertheless, this work was stimulated by, relies on, and agrees with the extensive body of work on hemostasis (14, 15, 17, 19–21, 27–31). There are two reasons these results may have *in vivo* relevance. (*i*) Simple *in vitro* experiments (e.g., prothrombin time and activated partial throm-

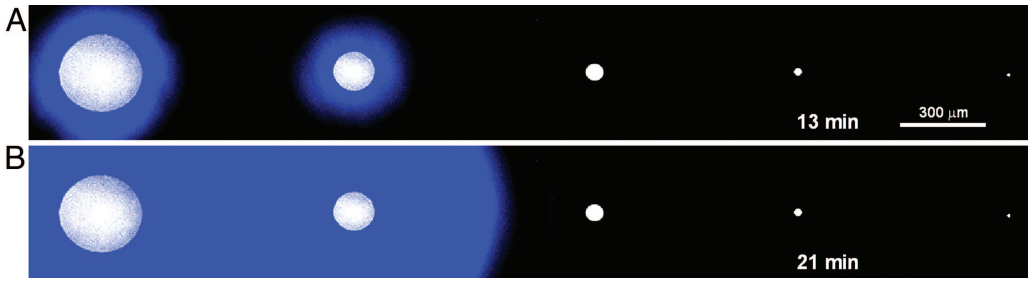

Fig. 4. Chemical model correctly predicts initiation of clotting via the factor XII pathway, suggesting that the model describes the dynamics of initiation of the entire complex network of hemostasis *in vitro*. Tests of initiation of clotting via the factor XII pathway in human blood plasma on glass is shown. Two time-lapse fluorescent micrographs at 13 (*A*) and 21 (*B*) min showing initiation of clotting (blue) on an array of clot-inducing hydrophilic glass patches $p = 400$, 200, 100, 50, and 25 μm (left to right, white) patterned in a background of inert silanized glass (black). For the blood plasma sample shown here, the threshold patch size was between 100 and 200 μm.

boplastin time clotting tests) are routinely used in healthcare to evaluate the function of a patient's clotting network and to monitor adequacy of anticoagulation therapy. (*ii*) We performed a number of additional preliminary experiments that mimic the *in vivo* system more closely and observed that the predictions of the chemical model still hold, at least under the specific conditions we have tested. These preliminary experiments included the incorporation of thrombomodulin (an integral membrane protein that inhibits clotting) into the inert bilayer, replacing normal pooled plasma (low platelet count) with platelet-rich plasma and whole blood, measurements at 37°C, and varying the TF concentration by a factor of 20. Preliminary results also indicated that enhanced removal of activator from the patch by convective flow, or changes in patch shape, increased p_{tr}. These preliminary experiments, although outside of the scope this article, must be used along with *in vivo* investigations (33) to establish the importance of this work to the function of hemostasis in the human body. If these results are relevant *in vivo*, they provide a potential resolution to the debate (20, 21, 46) on whether TF can circulate in blood without causing clotting. In the absence of damage, TF could circulate on individual microparticles that are below the threshold "patch" size. Recruitment and localization of TF-bearing microparticles to surfaces could construct a large patch that exceeds threshold and initiates clotting. The mechanism proposed here for blood clotting might also be relevant to other "all-or-none" systems that are initiated by surface-bound stimuli, such as T cell activation (34).

Here, we have tested whether spatiotemporal dynamics of a complex reaction network can be modeled by (*i*) separating the network into modules, (*ii*) building an experimental chemical network by replacing each module with a simple chemical reaction, and (*iii*) using microfluidics to probe (4) the dynamics of the chemical model and the biological network under similar conditions in space and time. Surprisingly, the simple chemical model was semiquantitatively predictive for initiation of blood clotting *in vitro*. Chemists have used simple mechanisms and synthetic model systems to understand reactivity of organic molecules (35) and function of enzymes (36–40). Chemical models have stimulated our understanding of spatiotemporal dynamics of a diverse range of nonequilibrium systems, including catalysis (41), oscillations in chemistry (3) and biology (42), oocyte development (1), and fibrillation in myocardium (43). Recently, several hundred molecular dimensions representing the complex apoptosis network have been correlated by mathematical data analysis to two fundamental dimensions describing most of the dynamics (44). Substantial evidence that biology is modular (1, 5, 6, 44, 45) provides additional motivation to test the generality of this approach to understand spatiotemporal dynamics of hemostasis and other complex reaction networks.

Materials and Methods

See the supporting information for detailed procedures and additional control experiments.

Preparing the Reagents of the Chemical Model. Two precursor solutions were prepared and combined in equal portions to form the metastable model reaction mixture (23). The two precursor solutions were (*i*) an aqueous solution containing $Na_2S_2O_3$ (0.492 mmol), alginic acid (5.8 mg/ml), and bromophenol blue (0.425 mM) (pH 7) and (*ii*) an aqueous solution containing $NaClO_2$ (2.99 mmol) (pH 10.7). Initiation of clotting in the chemical model consisted of $Na_2S_2O_3$ and $NaClO_2$ reacting to form a significant amount of H^+, which caused gelling of alginic acid and the transition of bromophenol blue to yellow, accompanied by quenching of red fluorescence. The photoacid-coated substrate was prepared by spin coating a 20- to 30-μm-thick layer of a dispersion of 2-nitrobenzaldehyde (50% by weight) in dimethylsiloxane-ethylene oxide block copolymer onto a siliconized coverslip. The microfluidic chamber used for the chemical model was constructed by sealing a poly(dimethylsiloxane) gasket to a siliconized coverslip. A 30-μl drop of the model reaction mixture was placed in the chamber, and the chamber was sealed to the photoacid substrate. A photomask allowed patches of UV light (300–400 nm) to contact the substrate only in specific locations, thus generating patches of acid. Epifluorescence microscopy was used to monitor the reaction mixture.

Numerically Simulating the Modular Mechanism of Initiation of Clotting on Surfaces Presenting Clotting Stimuli. Numerical simulations were used solely to illustrate that a threshold patch size can exist for the proposed modular mechanism, using a single rate equation to represent the kinetics of each module. The purpose was not to predict the exact size of the threshold patch. We believe that the time scale of reaction, t_R, a single experimentally determined parameter, is a simpler and more reliable predictor of the size of the threshold patch than a simulation. To simulate numerically the change in concentration of activator, C, we modeled the mass transport of C with the standard convection-diffusion equation using a commercial finite element package FEMLAB 3.1 (Comsol, Stockholm, Sweden). We used a diffusion coefficient of 5×10^{-11} $m^2 \cdot s^{-1}$ [approximate value for a solution-phase protease in blood clotting, such as thrombin (30)]. We considered diffusion and reactions occurring in the x,y dimensions in solution as well as at a surface patch surrounded by a 1-mm "inert" vicinity. In this pseudo-2D simulation, the z dimension was modeled by a single layer of 1-μm-thick mesh elements (1-μm boundary layer) (17). Three rate equations were incorporated into the simulation: (*i*) production of C at the surface of the patch, rate = k_{patch},; (*ii*) autocatalytic production of C in solution, rate = $k_{prod}[C]^2 + b$; and (*iii*) linear consumption of C in solution, rate = $-k_{consum}[C]$. The values used were $[C]_{initial} = 1 \times 10^{-9}$ M, $k_{patch} = 1 \times 10^{-9}$ $M \cdot s^{-1}$, $k_{prod} = 2 \times 10^7$ $M^{-1} \cdot s^{-1}$, $b = 2 \times 10^{-10}$ $M \cdot s^{-1}$, and $k_{consum} = 0.2$ s^{-1}. These values were selected based on approximate values (17) for representative reactions in blood clotting.

Patterning Substrates to Test Initiation of Clotting of Blood Plasma. Patterned substrates were prepared by using photolithography (26, 32). Glass coverslips were extensively cleaned and then made inert to clotting, either by forming a bilayer of phosphatidylcholine or a monolayer of hydrophobic silanes. In experiments testing the initiation of clotting through the TF pathway, a bilayer containing 1,2-dipalmitoyl-*sn*-glycero-3-phosphocholine (DPPC) with 3 mol % Oregon green 1,2-dihexadecanoyl-*sn*-glycero-3-phosphoethanolamine (Oregon green DHPE) was formed. In experiments testing initiation through the factor XII pathway, a monolayer of *n*-octadecyltrichlorosilane (OTS) was formed. The inert substrates were placed under a photomask (chrome on quartz) and irradiated with deep UV light. In experiments testing initiation via the TF pathway, the patterned DPPC bilayers were backfilled with TF-reconstituted vesicles (28) containing 1,2-dilauroyl-*sn*-glycero-3-phosphocholine (DLPC) (79.5 mol %), L-α-phosphatidylserine from porcine brain (PS) (20 mol %), Texas red 1,2-dihexadecanoyl-*sn*-glycero-3-phosphoethanolamine (Texas red DHPE) (0.5 mol %), and TF (TF:lipid ratio of 2.5×10^{-7}). Assuming that all TF incorporated into vesicles, the calculated surface concentration was 0.08 fmol/cm^2. For the patterned silanized substrates, hydrophilic regions were detected by a wetting test using glycerol.

Measuring Initiation of Clotting of Blood Plasma on Patterned Substrates. The microfluidic chambers used to contain blood plasma over the patterned substrates were constructed primarily from poly(dimethylsiloxane) fabricated from multilevel, machine-milled, brass masters. Pooled normal plasma (human) was purchased from George King Bio-Medical (Overland Park, KS).

Platelet-rich plasma and whole-blood samples were obtained from individual healthy donors in accordance with the guidelines set by the Institutional Review Board (Protocol No. 12502A) of University of Chicago. In experiments testing initiation via TF pathway, corn trypsin inhibitor was added to the plasma (100 μg/ml) to inhibit the factor XII pathway (29). Citrated blood plasma was recalcified and immediately placed on top of the substrate in the microfluidic chamber, and the chamber was sealed with a siliconized coverslip. Bright-field microscopy was used to detect the formation of fibrin, and fluorescence microscopy was used to detect thrombin-induced cleavage of a peptide-modified coumarin dye (29) (see the supporting information). The clot times reported here indicate the time that fibrin appeared, and in all experiments fibrin formation and increased fluorescence were correlated.

We thank Shaun R. Coughlin, Jay T. Groves, Satish Kumar, Yannis Kevrekidis, Daniel Koshland, Ka Yee Lee, Jonathan L. Miller, Atul Parikh, Thuong Van Ha, and Ding-Djung Yang for discussions and advice. This work was supported in part by National Science Foundation CAREER Award CHE-0349034 and Office of Naval Research Grant N00014-03-10482. M.K.R. was supported by Burroughs Wellcome Fund Interfaces ID 1001774. R.F.I. is a Cottrell Scholar of Research Corporation and an A. P. Sloan Research Fellow. Some of this work was performed at the Materials Research Science and Engineering Centers microfluidic facility (funded by the National Science Foundation).

1. Xiong W, Ferrell JE (2003) *Nature* 426:460–465.
2. Basu S, Gerchman Y, Collins CH, Arnold FH, Weiss R (2005) *Nature* 434:1130–1134.
3. Kurin-Csorgei K, Epstein IR, Orban M (2005) *Nature* 433:139–142.
4. Lucchetta EM, Lee JH, Fu LA, Patel NH, Ismagilov RF (2005) *Nature* 434:1134–1138.
5. Sprinzak D, Elowitz MB (2005) *Nature* 438:443–448.
6. Hartwell LH, Hopfield JJ, Leibler S, Murray AW (1999) *Nature* 402:C47–C52.
7. Koshland DE (1998) *Science* 280:852–853.
8. Vlad MO, Arkin A, Ross J (2004) *Proc Natl Acad Sci USA* 101:7223–7228.
9. Sakurai T, Mihaliuk E, Chirila F, Showalter K (2002) *Science* 296:2009–2012.
10. Wolff J, Papathanasiou AG, Kevrekidis IG, Rotermund HH, Ertl G (2001) *Science* 294:134–137.
11. Olofsson J, Bridle H, Sinclair J, Granfeldt D, Sahlin E, Orwar O (2005) *Proc Natl Acad Sci USA* 102:8097–8102.
12. Editorial (2002) *Nature* 416:247.
13. Whitesides GM, Ostuni E, Takayama S, Jiang XY, Ingber DE (2001) *Annu Rev Biomed Eng* 3:335–373.
14. Basmadjian D, Sefton MV, Baldwin SA (1997) *Biomaterials* 18:1511–1522.
15. Beltrami E, Jesty J (2001) *Math Biosci* 172:1–13.
16. Davies MJ (1997) *N Engl J Med* 336:1312–1314.
17. Kuharsky AL, Fogelson AL (2001) *Biophys J* 80:1050–1074.
18. Runyon MK, Johnson-Kerner BL, Ismagilov RF (2004) *Angew Chem Int Ed* 43:1531–1536.
19. Beltrami E, Jesty J (1995) *Proc Natl Acad Sci USA* 92:8744–8748.
20. Butenas S, Mann KG, Bogdanov VY (2004) *Nat Med* 10:1155–1156.
21. Morrissey JH (2003) *J Thromb Haemostasis* 1:878–880.
22. Bird RB, Stewart WE, Lightfoot EN (2002) *Transport Phenomena* (Wiley, New York), 2nd Ed.
23. Nagypal I, Epstein IR (1986) *J Phys Chem* 90:6285–6292.
24. Barth A, Corrie JET (2002) *Biophys J* 83:2864–2871.
25. Groves JT, Boxer SG (2002) *Acc Chem Res* 35:149–157.
26. Yee CK, Amweg ML, Parikh AN (2004) *J Am Chem Soc* 126:13962–13972.
27. van 't Veer C, Mann KG (1997) *J Biol Chem* 272:4367–4377.
28. Contino PB, Hasselbacher CA, Ross JBA, Nemerson Y (1994) *Biophys J* 67:1113–1116.
29. Lo K, Diamond SL (2004) *Thromb Haemostasis* 92:874–882.
30. Krasotkina YV, Sinauridze EI, Ataullakhanov FI (2000) *Biochim Biophys Acta* 1474:337–345.
31. Mann KG, Nesheim ME, Church WR, Haley P, Krishnaswamy S (1990) *Blood* 76:1–16.
32. Howland MC, Sapuri-Butti AR, Dixit SS, Dattelbaum AM, Shreve AP, Parikh AN (2005) *J Am Chem Soc* 127:6752–6765.
33. Falati S, Gross P, Merrill-Skoloff G, Furie BC, Furie B (2002) *Nat Med* 8:1175–1180.
34. Mossman KD, Campi G, Groves JT, Dustin ML (2005) *Science* 310:1191–1193.
35. Whitesides GM, Ismagilov RF (1999) *Science* 284:89–92.
36. Benkovic SJ, Hammes-Schiffer S (2003) *Science* 301:1196–1202.
37. White MC, Doyle AG, Jacobsen EN (2001) *J Am Chem Soc* 123:7194–7195.
38. Goldbeter A, Koshland DE (1981) *Proc Natl Acad Sci USA* 78:6840–6844.
39. Tshuva EY, Lippard SJ (2004) *Chem Rev* 104:987–1011.
40. Halpern J, Kim SH, Leung TW (1984) *J Am Chem Soc* 106:8317–8319.
41. Cirak F, Cisternas JE, Cuitino AM, Ertl G, Holmes P, Kevrekidis IG, Ortiz M, Rotermund HH, Schunack M, Wolff J (2003) *Science* 300:1932–1936.
42. Goldbeter A, Dupont G, Berridge MJ (1990) *Proc Natl Acad Sci USA* 87:1461–1465.
43. Winfree AT (1994) *Science* 266:1003–1006.
44. Janes KA, Albeck JG, Gaudet S, Sorger PK, Lauffenburger DA, Yaffe MB (2005) *Science* 310:1646–1653.
45. Kashtan N, Alon U (2005) *Proc Natl Acad Sci USA* 102:13773–13778.
46. Hathcock J, Nemerson Y (2004) *Nat Med* 10:1156